# Multi-Object Optimization of the Switched Reluctance Motor

**Jae-Hak Choi*, Sol Kim*, Yong-Su Kim*, Sang-Don Lee** and Ju Lee†**

**Abstract** - In this paper, multi-object optimization based on a progressive quadratic response surface method (PQRSM) and a time stepping finite element method (FEM) is proposed. The new PQRSM and FEM are able to decide optimal geometric and electric variables of the switched reluctance motor (SRM) with two objective functions: torque ripple minimization and average torque maximization. The result of the optimum design for SRM demonstrates improved performance of the motor and enhanced relationship between torque ripple and average torque.

**Keywords**: average torque, multi-object optimization, switched reluctance motor, torque ripple

## 1. Introduction

The switched reluctance motor (SRM) has numerous advantages such as simple and rugged motor construction, high reliability, and low cost. Due to these advantages, use of the SRM in many industrial fields has been rapidly increasing over the last ten years [1]. However, the SRM also has some problems that limit its applications because of its inherent structure, one of which is the torque ripple that causes undesirable acoustic noise and high vibration. The torque ripple fundamentally depends upon geometric variables that are relative to a stator pole arc ( $\beta_s$ ) and a rotor pole arc ( $\beta_r$ ). The design schemes that determine optimal geometric variables ( $\beta_s$ and $\beta_r$ ) to reduce the torque ripple of the SRM have been reported in various papers [2-5]. However, the proposals did not take into account an influence of electric variables, that is, a turn-on angle ( $\theta_{on}$ ) and a turn-off angle ( $\theta_{off}$ ), when achieving the geometric design optimization on a single objective function such as simply minimizing the torque ripple.

As the application field of the SRM is quite diversified, the torque performance and the acceptable range of torque ripple demanded in its practical use grow to be different. It is actually known that there exists a trade-off relationship between the torque ripple and the average torque. For that reason, it is necessary to study an approach that determines optimal geometric and electric variables ( $\beta_s$ , $\beta_r$ , $\theta_{on}$ , and $\theta_{off}$ ) for minimizing the torque ripple on the average torque specified according to the SRM applications.

In this paper, the multi-object optimization that is able to decide optimal design variables ( $\beta_s$ , $\beta_r$ , $\theta_{on}$ , and $\theta_{off}$ ) being satisfied by both a torque ripple minimization and an average torque maximization is presented. The optimal design has been obtained based on the time stepping finite element method (FEM) [6] and progressive quadratic response surface method (PQRSM) [7-9]. As all design variables have a mutually subordinate relationship, the conventional gradient-based nonlinear optimizing method (CGM) that considers the variables as discrete variables is unable to be used. In this work, we utilize the PQRSM as the optimization algorithm for coping with this difficulty. This method approximates objective and constraint functions to quadratic functions within a reasonable design space and sequentially optimizes approximate optimization problems in the context of the trust region model management strategy. In order to perform the feasibility study of this optimization, optimal design variables and performance of the SRM on multi-object function are investigated.

## 2. Switched Reluctance Motor

### 2.1 Research Model

Fig. 1 depicts a cross section of the 6/4 SRM and drive circuit, which is designed for automotive accessories. $\beta_s$ and $\beta_r$ represent stator pole arc and rotor pole arc, respectively. The motor drive consists of an asymmetric bridge converter. For the driving of the SRM, each phase is sequentially operated. Table 1 presents the basic specifications of the research model.

* Dept. of Electrical Engineering, Hanyang University, Korea. (ivy@ihanyang.ac.kr)
** Dept. of Electrical Engineering, Wonju National College, Korea. (leesd@wonju.ac.kr)
† Corresponding author: Dept. of Electrical Engineering, Hanyang University, Korea. (julee@hanyang.ac.kr)
Received April 13, 2004 ; Accepted October 30, 2004

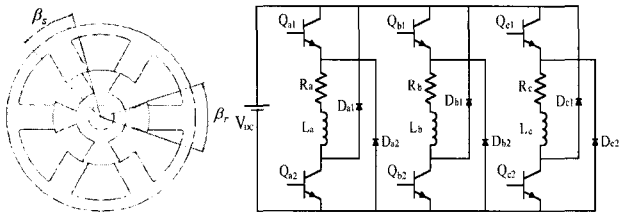

**Fig. 1** Cross section of switched reluctance motor and drive circuit

**Table 1** Basic Specifications of the Research Model

| stator/rotor poles | 6/4 | stack length | 40 (mm) |
|---|---|---|---|
| number of phases | 3 | air-gap | 0.3 (mm) |
| stator outer diameter | 100 (mm) | rated speed | 500 (rpm) |
| stator inner diameter | 40.6 (mm) | rated current | 4 (A) |
| rotor outer diameter | 40 (mm) | DC-link voltage | 12 (V) |
| rotor inner diameter | 8 (mm) | number of turns | 79 |

## 2.2 Design Variables

The instant motor torque ($T$) is calculated by derivative of the inductance ($L$), which is a function of rotor position ($\theta$), as shown in (1)

$$T(\theta, i) = 1/2 \cdot i^2 \cdot dL(\theta)/d\theta . \quad (1)$$

Although the derivative of inductance is constant, constant torque cannot be obtained because of the electrical time constant. Therefore, the turn-on and turn-off according to variation of inductance should be considered to improve the torque ripple and the average torque.

When the rotor teeth are unaligned with the stator teeth, the angle is set to 0° (mechanical degree). When the rotor teeth are aligned with the stator teeth, the angle is set to 45°. Inductance profile varies with the combination of stator and rotor pole arcs, and influences the torque performances. For minimum torque ripple and maximum average torque, the pole arcs of the stator and rotor have to be more than 30°. If the pole arcs of the stator and rotor are smaller than 30°, a large torque ripple will be periodically generated. It is also impossible to reduce torque ripple although the phase current flows ideally.

Fig. 2 indicates inductance profile, switching current and torque characteristic when $\beta_s$ =30° and $\beta_r \geq 30°$. To widen the pole arc of the rotor is better than to widen the pole arc of the stator with respect to space factor, magneto motive force and average torque. As shown in Fig. 2, torque ripple is ideally able to be zero while increasing average torque. Consequently, the pole arcs of the rotor and stator, turn-on angle and turn-off angle among electric and geometric variables are selected as design variables for optimization.

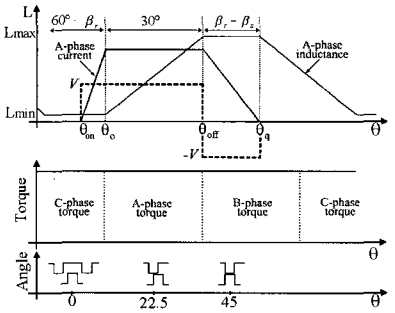


**Fig. 2** Illustration of torque generation principles with pole arc combination when $\beta_s$ =30° and $\beta_r \geq 30°$

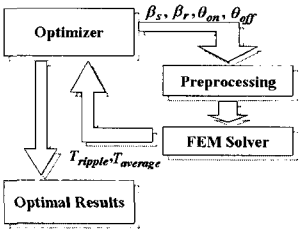


**Fig. 3** The optimization procedure

## 3. Progressive Quadratic Response Surface Method

Fig. 3 illustrates the optimal design process used in this paper. As shown in Fig. 3, $\beta_s$, $\beta_r$, $\theta_{on}$, and $\theta_{off}$ are adopted as design variables to obtain optimal results. To calculate the object functions, two-dimensional time stepping FEM considering the driving circuit is used. The multi-object function, constraints and design variables are represented by (2).

Multi-object Function: Maximize average torque and minimize torque ripple,

$T_{minimize} = -\alpha_1 (T_a / T_a') + \alpha_2 (T_r / T_r')$,

Constraints on: One maximum phase current,

$I_{max} \leq 6$(A),

Design variables:

$$-15° \leq \theta_{on} \leq 15°, \; 30° \leq \theta_{off} \leq 45°,$$
$$\beta_s = 30°, \; 30° \leq \beta_r < 60°, \quad (2)$$

where $\alpha_1$ and $\alpha_2$ are weight, $(T_a / T_a')$ is the normalized average torque, and $(T_r / T_r')$ is the normalized torque ripple

In this study, conventional gradient-based nonlinear optimization algorithms like the Conjugate Gradient Method (CGM) cannot be used because all design variables are considered as discrete variables. To overcome this difficulty, we used PQRSM for the optimization algorithm. This method approximates objective and constraint functions to quadratic functions within the

reasonable design space and sequentially optimizes the approximate optimization problems in the context of the trust region model management strategy. The trust region model management strategy adaptively restricts design moves within trust regions, where the approximate function produces information that agrees with the actual function within an acceptable tolerance to error. Because PQRSM only utilizes objective and constraint functions to build approximate functions and does not use gradient information like other conventional response surface methods, it is a very useful system when employed for problems where gradient information cannot be obtained.

PQRSM has the following two merits compared with conventional response surface methods. First, PQRSM is a very efficient function based on an approximate method. It requires only $2n+1$ ($n$ is the number of design variables) sampling points for constructing a quadratic approximate function. Conversely, the conventional response surface methods need at least $(n+1)(n+2)/2$ sampling points to construct a quadratic response surface function. Second, PQRSM uniquely determines the regression coefficients despite the fact that conventional response surface methods use least square methods to determine the regression coefficients. Thus, PQRSM does not require the additional CPU time to construct an approximate function explicitly.

Fig. 4 describes the algorithm flowchart of the PQRSM. The computational procedure of the PQRSM is as follows: Step 0; Set the initial design and the design space. The initial design space is assumed to be 50% ~ 100% of the entire design space, including the initial design. Step 1; Select 2n+1 sampling points within the design space. The sampling points set consists of the initial design point and newly selected 2n design points along the design variable axes. Step 2; Approximate the objective and constraints functions to quadratic polynomial functions. Step 3; Find an approximate optimum using the approximate objective and constraint functions. Step 4; Evaluate actual objective and constraints at the approximate optimum by real analysis. Step 5; Check convergence at the approximate optimum using actual objective and constraints function values. If the approximate optimization problem is converged, then terminate the optimization. Otherwise adjust the design space by a trust region concept [10]. Step 6; Select 2n+1 design points within the new design space. The sampling points set consists of one previously calculated points set and newly selected 2n design points. Go to Step 2.

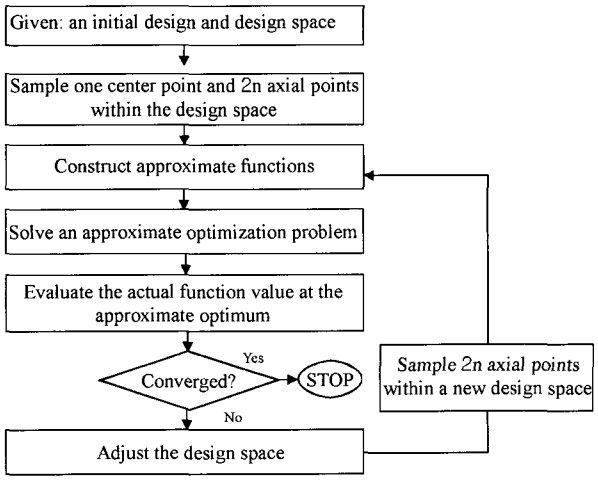


**Fig. 4** Progressive quadratic response surface method algorithm

## 4. Finite Element Method

If the magnetic vector potential and current density have only a $z$-axis component, the governing equation for SRM can be expressed in a magnetic vector potential $A$ as follows:

$$\frac{\partial}{\partial x}\left(\nu\frac{\partial A}{\partial x}\right)+\frac{\partial}{\partial y}\left(\nu\frac{\partial A}{\partial y}\right)+J_o=0, \tag{3}$$

where ν is the inverse of permeability, $A$ is the magnetic vector potential, and $J_0$ is the input current density. The electrical input equation of the voltage source is expressed as

$$V=R_m I_m+E_m, \tag{4}$$

where $V$ is the voltage source, $R_m$ is the phase resistance, $I_m$ is the phase current, and $E_m$ is the electromotive force induced in the coil. After applying the Galerkin method in (3) and coupling the voltage equation (4), the system matrix equation is obtained by using the time difference scheme as follows.

$$\begin{bmatrix}[s] & [Q]\\ 1/\Delta t[F] & [R_m]\end{bmatrix}\begin{bmatrix}A^{t+\Delta t}\\ I_m^{t+\Delta t}\end{bmatrix}=\begin{bmatrix}0 & 0\\ 1/\Delta t[F] & 0\end{bmatrix}\begin{bmatrix}A^{t}\\ I_m^{t}\end{bmatrix}+\begin{bmatrix}0\\ V^{t+\Delta t}\end{bmatrix} \tag{5}$$

## 5. Optimal Design Results

Table 2 indicates that a high torque ripple and a low average torque are generated in the initial model. However, Table 3 shows the improved torque characteristics of the optimal model in both object functions according to the variation of weight ($\alpha_1$ and $\alpha_2$). As presented in Table 3, when weight $\alpha_1$ is 1.0 and $\alpha_2$ is 0.0, the average torque of the optimal model is increased 2-fold with respect to the initial model. The torque ripple is also decreased by 15

times with respect to the initial model, when weight $\alpha_1$ is 0.0 and $\alpha_2$ is 1.0.

**Table 2** Initial design variables and objective functions

| | | | |
|---|---|---|---|
| average torque ($T_a$) | 2.9kg.cm | torque ripple ($T_r$) | 88.4% |
| stator pole arc ($\beta_s$) | 30° | turn-on ($\theta_{on}$) | 8.0° |
| rotor pole arc ($\beta_r$) | 30° | turn-off ($\theta_{off}$) | 32.9° |
| One maximum phase current ($I_{max}$) | 4.4(A) | | |

**Table 3** Optimal design results and objective functions

| $\alpha_1$ | $\alpha_2$ | $\beta_s$ | $\beta_r$ | $\theta_{on}$ | $\theta_{off}$ | Imax (A) | Ta kg.cm | Tr (%) |
|---|---|---|---|---|---|---|---|---|
| 1.0 | 0.0 | 30° | 48.8° | -4.9° | 35.6° | 5.99 | 3.94 | 51.6 |
| 0.9 | 0.1 | 30° | 50.3° | -0.5° | 36.3° | 4.60 | 2.84 | 6.93 |
| 0.7 | 0.3 | 30° | 50.6° | -0.7° | 36.4° | 4.60 | 2.82 | 6.31 |
| 0.5 | 0.5 | 30° | 50.6° | -0.5° | 36.4° | 4.61 | 2.81 | 6.24 |
| 0.3 | 0.7 | 30° | 50.7° | -0.7° | 36.1° | 4.61 | 2.80 | 6.29 |
| 0.1 | 0.9 | 30° | 50.6° | -0.5° | 35.8° | 4.50 | 2.80 | 6.25 |
| 0.0 | 1.0 | 30° | 50.6° | -0.5° | 36.4° | 4.61 | 2.79 | 6.19 |

Fig. 5 illustrates the inductance and current characteristics of the initial model. In the initial model, negative phase torque is not produced because the phase current becomes zero before the falling-inductance period.

Fig. 6 also shows the inductance and current characteristics of the optimal model. In the optimal model, negative phase torque is not produced because the phase current becomes zero prior to the inductance decrease.

Fig. 7 indicates the energy conversion loop of the initial model and the optimal model. Estimation for the average torque could be illuminated with areas on the energy conversion loop. It can be known that the average torque of the optimal model is much higher than that of initial the model.

Fig. 8 and Fig. 9 depict the total torque characteristics comparison between the initial model and the optimal model. The torque ripple of the initial model is very large, at almost 88.4%, as shown in Table II. Fig. 9 also displays that of the optimal model for minimizing torque ripple. As shown in Table III, when $\alpha_1$ is 0.0 and $\alpha_2$ is 1.0, the torque ripple of the optimal model is drastically improved to 6.2%. It can be known that the torque ripple and average torque were satisfied of their constraint conditions and there was a trade-off between the torque ripple and the average torque.

## 6. Conclusion

This paper presented the results of this optimum design for maximizing the average torque and minimizing torque ripples specified according to the SRM applications. In that work, the time stepping FEM has been effectively used in taking the drive circuit and the switching condition into account. In order to identify approaches to the SRM, optimal design variables as well as performances were investigated in detail. A trade-off characteristic between the average torque and the torque ripple was also investigated. The optimal design process proposed in this article may also be used effectively for various electric machines.

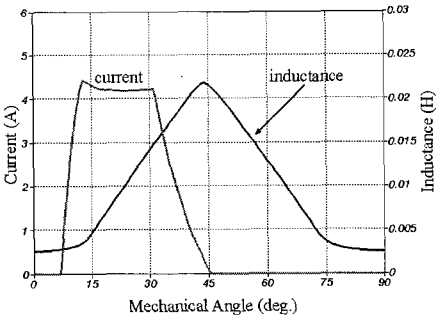


**Fig. 5** Current and inductance in initial model

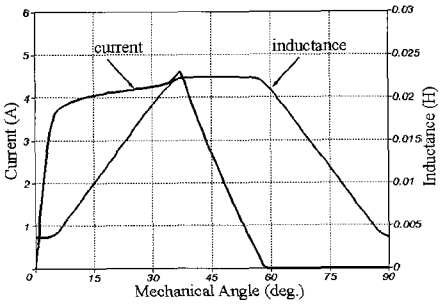


**Fig. 6** Current and inductance in optimal model

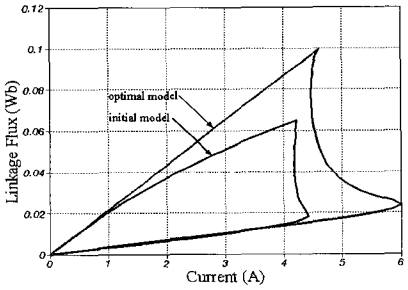


**Fig. 7** Average torque; Energy conversion loop

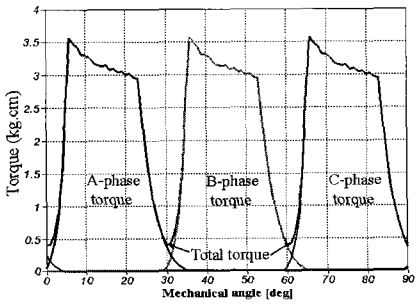


**Fig. 8** Torque ripples of initial model

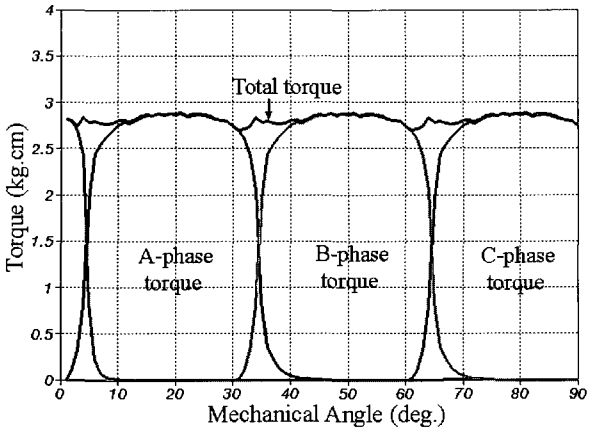


**Fig. 9** Torque ripples of optimum model

## Acknowledgements

This work was financially supported by both MOCIE through the EIRC program and by the Korea Electrical Engineering & Science Research Institute under grant R-2004-B-125, which is funded by the Ministry of Commerce, Industry and Energy.

## References

[1] T. J. E. Miller, *Switched Reluctance Motors and their control,* Hillsboro, OH: Magna Physics Publishing and London: Oxford University Press, 1993, pp. 1-23.

[2] W. F. Ray, P. J. Lawrenson, R. M. Davis, J. M. Stephenson, N. N. Fulton, and R. J. Blake, "High performance switched reluctance brushless drives," *IEEE Trans. Ind. Applicat.,* vol. IA-22, no. 4, pp. 722-730, 1986.

[3] Y. Ohdachi and Y. Kawase, "Optimum Design of Switched Reluctance Motors using Dynamic Finite Element Analysis," *IEEE Trans. on Magn.,* vol. 33, pp. 2033-2036, March 1997.

[4] Funda Şahin, H. Bülent Ertan, and Kemal Leblebicioğlu, "Optimum Geometry for Torque Ripple Minimization of Switched Reluctance Motors," *IEEE Trans. on Energy conversion,* vol. 15, no. 1, pp. 30-39, March 2000.

[5] S. Brisset and P. Brochet, "Optimization of Switched Reluctance Motors using Deterministic Methods with Static and Dynamic Finite Element Simulation," *IEEE Trans. on Magn.,* vol. 34, pp. 2853-2856, September 1998.

[6] Y. –H. Kim, J, -H. Choi, S. –I. Jung, Y. –D. Chun, J. Lee, M. –S. Chu, K. –J. Hong, and D. -H. Choi, "Optimal design of switched reluctance motor using two-dimensional finite element method," *Journal of Applied Physics*, vol. 91, no. 10, pp. 6967, May 2002.

[7] Jasbir S. Arora, *Introduction To Optimum Design*, Mcgraw-Hill International Editions, 1994.

[8] K. -J. Hong, Ph. D. Thesis, "Trust Region Managed Sequential Approximate Optimization with Response Surface Modeling," Hanyang University, Korea, 2001.

[9] K. -J. Hong, M. -S. Kim, and D. -H. Choi, "Efficient Approximation Method for Constructing Quadratic Response Surface Model," *KSME International Journal*, vol. 15, no. 7, pp. 876, 2001.

[10] Fletcher, R., *Practical Method of Optimization*, John Wiley & Sons, Chichester, 1987.

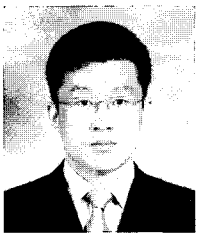

**Jae-Hak Choi**
He received his B.S. and M.S. degrees in Electrical Engineering from Hanyang University in 1999 and 2001, respectively. He is currently enrolled in a doctorate course in the Department of Electrical Engineering, Hanyang University, Seoul, Korea. His research interests are the design and analysis of motors.

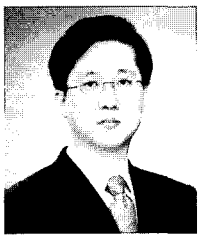

**Sol Kim**
He was born in Seoul, Korea in 1970. He received his B.S., M.S. and Ph.D degrees in Electrical Engineering from Hanyang University in 1997, 1999 and 2004, respectively. He is a Principal Researcher at HCEM, Hanyang University, Seoul, Korea. He is a member of KIEE, IEEE, and IEC/TC2.

**Yong-Su Kim**
He received his B.S. and M.S. degrees in Electrical Engineering from Hanyang University in 1993 and 1995, respectively. He is enrolled in a doctorate course in the Department of Electrical Engineering, Hanyang University, Seoul, Korea. His research interests are the design and analysis of motors.

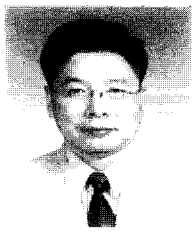

**Sang-Don Lee**

He received his B.S., M.S. and Ph.D degrees in Electrical Engineering from Hanyang University in 1981, 1987 and 1996, respectively. He was a Senior Researcher at the Agency for Defense Development from 1988 to 1995. He was a Visiting Professor at Simon Fraser University, Canada from 2003 to 2004. Currently, he is a Professor in the Department of Electrical Engineering, Wonju National College, Gangwondo, Korea.

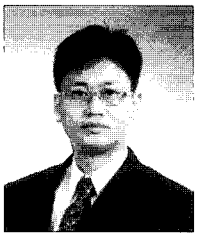

**Ju Lee**

He received his B.S. and M.S. degrees in Electrical Engineering from Hanyang University in 1986 and 1988, respectively. He received his Ph.D degree in Electrical Engineering at Kyu-Shu University, Japan in 1997. He was a Researcher at the Agency for Defense Development from 1988 to 1993. He was a Head Researcher at the Korea Railroad Research Institute in 1997. Currently, he is an Associate Professor in the Division of Electrical and Computer Engineering, Hanyang University, Seoul, Korea.